HHS Public Access

Author manuscript

Nature. Author manuscript; available in PMC 2020 April 16.

Published in final edited form as:

Nature. 2019 November ; 575(7784): 643–646. doi:10.1038/s41586-019-1690-5.

Concise Asymmetric Synthesis of (–)-Bilobalide

Meghan A. Baker[1,‡], **Robert M. Demoret**[1,‡], **Masaki Ohtawa**[1,†,*], **Ryan A. Shenvi**[1,*]

[1]Department of Chemistry, The Scripps Research Institute, 10550 North Torrey Pines Road, La Jolla, California 92037, United States.

The *Ginkgo biloba* metabolite bilobalide is widely ingested by humans but its effect on the mammalian central nervous system is not fully understood[1,2,3,4]. Antagonism of *gamma*-aminobutyric acid A receptors ($GABA_A$Rs) by bilobalide has been tied to rescue of cognitive deficits in mouse models of Down syndrome[5]. A lack of convulsant activity coupled with these neuroprotective effects have led some to postulate an alternative, unidentified target.[4] However, steric congestion and the instability of 1[1,2,6] have prevented pulldown of biological targets other than the $GABA_A$Rs. A concise and flexible synthesis of 1 would provide a platform to generate probes for identification of potential new targets; analogs with differential selectivity between insect and human $GABA_A$Rs; and stabilized analogs with enhanced serum half-life[7]. Here we exploit the unusual reactivity of bilobalide to affect a late-stage oxidation that symmetrizes the molecular core and allows oxidation states to be embedded in the starting material. The same overall strategy disclosed here may be applicable to *G. biloba* congeners including the ginkgolides, some of which are glycine receptor (GlyR)-selective antagonists[8]. The therapeutic potential of bilobalide and its incompletely understood effects can now be interrogated through chemical synthesis.

*Correspondence should be addressed to M.O. (ohtawam@pharm.kitasato-u.ac.jp) or R.A.S. (rshenvi@scripps.edu) and requests for materials should be addressed to R.A.S.

†Present Address: Graduate School of Pharmaceutical Sciences, Kitasato University, 5-9-1, Shirokane, Minato-ku, Tokyo 108-8641, Japan

‡These authors contributed equally to this work.

Author Contributions R.A.S, M.A.B, R.M.D and M.O. conceived the project. R.A.S. directed the research, and R.A.S., M.O., M.A.B. and R.M.D. composed the manuscript and the Supporting Information section. M.O., M.A.B. and R.M.D. completed a first-generation synthesis of *rac*-**1**. M.A.B. conceived and developed the catalytic asymmetric synthesis of (–)-**7**. M.A.B. observed, designed and optimized the parallel kinetic resolution of *rac*-**9**. M.O. and R.M.D. screened and optimized conditions for the alkyne oxidation of *rac*-**12** and (+)-**12**. R.M.D. developed the hydration of *rac*-**8** and (–)-**8** and optimized scale-up campaigns of *rac*-**5** and (–)-**5**. M.A.B. and R.M.D. conducted large-scale syntheses of *rac*-**5** and (–)-**5**. M.A.B. and R.M.D. investigated the rearrangement of *rac*-5 and (–)-5 to 16a–c. M.O. discovered an oxidation of *rac*-**5** to *rac*-**1**. M.A.B. investigated the rearrangement of *rac*-**5** and (–)-**5** to **16b** and **16c**, and discovered conditions that were utilized for the oxidation of *rac*-**5** and (–)-**5** to *rac*-**1** and (–)-**1**; M.A.B. and R.M.D. both optimized this process.

Data and materials availability: All data is made available in the main text or the Supplementary Information. Structural parameters are available from the Cambridge Crystallographic Data Centre: (–)-**5** (CCDC1911131), (–)-**8** (CCDC1911128), **12** (CCDC1911129), and **16c** (CCDC1911127). The authors declare no competing financial interest.

The authors declare no competing financial interests.

Readers are welcome to comment on the online version of the paper.

Supplementary Information is available in the online version of this paper.

Reviewer information *Nature* thanks the anonymous reviewers for their contribution to the peer review of this work.

The leaves of *Ginkgo biloba* have been used historically as insecticides and helminthicides[9,10], activity attributed to its constituent terpene trilactones, including bilobalide (**1**, Fig. 1)[11,12]. *Ginkgo* extracts have seen use in traditional Chinese medicine to treat senility, a practice that has penetrated the Western world, albeit controversially, due to opposing claims of efficacy[1] and serious adverse effects associated with Ginkgo toxin (4-*O*-methylpyridoxine)[2] or inhibition of platelet aggregating factor (PAF)[13] by ginkgolides. Animal models demonstrate some credible effects on impaired cognition: Down syndrome model mice (Ts65DN), which show deficits in declarative learning and memory, exhibit normalized novel object recognition after treatment by pure bilobalide[5]. Rescue of learning and memory is proposed to arise through neuronal excitation by antagonism of $GABA_A$Rs. Unlike the plant metabolite picrotoxinin (**2**, Figure 1), bilobalide is not acutely toxic, and unlike the gingkolides, bilobalide does not affect PAF. Despite their disparate toxicity, bilobalide and picrotoxinin exhibit similar inhibitory potencies at recombinant $GABA_A$Rs (IC_{50} = 4.6 μM vs. 2.0 μM, respectively; $\alpha_1\beta_2\gamma_{2L}$, *Xenopus laevis* oocytes), but differentially inhibit the actions of $GABA_A$R positive modulators[14].

In addition to incomplete approaches[15–16, 17], two prior syntheses of bilobalide have been completed [24 steps enantioselective;[18,19]17 steps racemic[20]], both of which established the cyclopentane core with efficiency but required 8–11 subsequent redox steps to reach the target. Guided by these challenges, we realized that a single oxidation transform might reduce synthetic complexity by unmasking a pseudosymmetric fused dilactone, ultimately leading to a symmetric starting material (see Figure 1). However, late-stage installation of the deep C10 hydroxyl (Figure 1, highlighted in red) presented a problem. Neither hydrogen of its precursor inner-lactone (shown in green) seemed accessible, whereas a hydrogen of the outer-lactone (shown in blue) resided at the surface of bilobalide's bowl-like scaffold. Here, we utilize unexpected properties of the bilobalide scaffold in a concise synthesis of (–)-*des*-hydroxybilobalide (>99% *ee,* **5**, Figure 1), which relies on stereocontrol transmitted from an unusual oxetane acetal. A late-stage oxidation is rendered regioselective using skeletal rearrangement and acidification, completing the synthesis of (–)-bilobalide in a single additional step.

The synthesis commenced with a methodological challenge: an asymmetric Reformatsky reaction between **6a** and **6b** (available in two and one steps respectively, see SI section 3). Reformatsky conditions proved necessary due to the tendency of **7** to undergo retro-aldol cleavage under basic conditions, whereas zinc, chromium and samarium alkoxides were stable at −78 °C. There have been no examples of catalytic enantio- and diastereoselective zinc Reformatsky reactions[21], nor use of simple, chiral L-type bisoxazoline (BOX) ligands. Wolf has demonstrated the use of related, electron-rich hemiaminals to control single stereocenters[22], and the simplicity of these conditions provided a foundation to explore. After a ligand screen, we found that a combination of diethylzinc and indabox (10 mol% A) were effective to provide secondary alcohol **7** in 97:3 *er* in favor of *syn*-diastereomer **7** (2.3:1). The combined yield of both diastereomers was determined to be 64% by NMR (purification by chromatography on silica led to material loss via retro-aldol), and the crude reaction mixture could be carried forward efficiently. The doubly-activated bromide **6a** may

uniquely enable the use of simple BOX ligands, which have eluded use for enantioselective Reformatsky reactions[21].

A Giese-type 5-*exo*-trig cyclization of **7** occurred with high regio- and diastereoselectivity (20:1 dr; 6-*endo*-trig n.d.) to form the quaternary carbon of cyclopentene **8**. Recrystallization purified the material to >99% enantiomeric excess and provided the product in 21% yield over two steps; the relative and absolute stereochemistry were confirmed by x-ray crystallography (see SI section 5).

Prior syntheses of **1** installed the extremely hindered *tert*-alkyl, bis-*neo*-pentyl C8 hydroxyl either by late-stage dihydroxylation with stoichiometric osmium tetroxide (23 °C, 12 hr)[18]; or by early-stage nitrile anion addition to a *tert*-butyl ketone, which rendered the synthesis racemic[20]. More recently, the Drago-Mukaiyama hydration has emerged as an effective method to chemoselectively hydrate hindered alkenes through an outer-sphere, metal-hydride hydrogen atom transfer (MHAT) mechanism[23]. In this case, application of standard conditions delivered a low-yield of **9** with no diastereoselectivity (Figure 2b, entry 4). We recently discovered that the kinetically-relevant reductant in many Mukaiyama reactions is an alkoxysilane (e.g. Ph(*i*-PrO)SiH_2) formed *in situ* by silane alcoholysis[24]. This custom, commercially available silane allowed us to screen a diverse range of solvents, and we identified a correlation between solvent polarity and diastereoselectivity, possibly due to internal hydrogen bonding (see Figure 2b). Ligands on the metal catalyst had no effect on dr. *Tert*-butylmethyl ether favored the wrong *(S)*-C8 diastereomer of the alcohol (which cyclized to a lactone), whereas methylcyclohexane reversed this stereoselectivity to favor *(R)*-C8 diastereomer **9** in a 3:1 ratio.

Formation of the fourth contiguous, fully-substituted carbon atom by alkylation was frustrated by dehydration of **9** under basic conditions or preference for the wrong C5 stereoisomer. Surprisingly, treatment of **9** with strong acid led to unexpectedly stable oxetane acetals **10** (*endo*-OMe) and **11** (*exo*-OMe), possibly driven by a 'corset effect' that increases the barrier to ring-opening of strained molecules like tetrahedranes[25]. Only the minor *endo*-isomer **10** could be carried forward: the major *exo*-OMe diastereomer **11** dehydrated under basic conditions and its epimerization to **10** was unsuccessful. However, analysis by chiral chromatography indicated that a moderate parallel kinetic resolution of (*rac*)-**9** had occurred: each diastereomer possessed opposite enantiomeric excess [39:61 er versus 69:31 er]. Accordingly, a single enantiomer of **9**, if matched with the correct enantiomer of chiral acid, would favor formation of the desired *endo*-**10**. Indeed, whereas (–)-**9** reacted with (–)-**B** to favor (1.4:1) *exo*-acetal **11**, (+)-**9** reacted to favor (4.5:1) *endo*-acetal **10**, isolated in 71% yield as a single enantiomer. *Endo*-acetal **10** proved crucial to control formation of the final quaternary carbon.

Due to steric hindrance in substrate **10**, the final C–C bond could only be established using an alkyne electrophile. A 3-step sequence was run in quick succession due to intermediate instability; only alkyne **12** could be purified. First, 2-iodoxybenzoic acid (IBX) oxidation delivered an unstable β-keto ester that could undergo α-alkylation. Second, this mixture of keto-enol tautomers was treated with Waser's reagent (TMS-EBX) and tetra-*n*-butylammonium fluoride (TBAF)[26]. The *endo*-methoxy oxetane effectively shielded one

trajectory of electrophile approach and provided the product as a single diastereomer. In contrast, the *exo*-methoxy oxetane, if carried forward to this step, eliminated the *tert*-alkyl ether and did not undergo alkynylation. Alkynylation prior to oxetane formation delivered exclusively the incorrect diastereomer. The unstable alkynylation product was reduced with high stereoselectivity using SmI_2 in a mixture of tetrahydrofuran/water to provide the stable alcohol **12** in 60% yield over 3 steps.[27] Traditional hydride reductants produced the opposite diastereomer. Anti-Markovnikov hydration of the alkyne to directly incorporate the northern lactone motif could not be accomplished under a variety of standard conditions including oxidation by lithium *tert*-butylperoxide[28], so an alternative procedure was developed. Deprotonation of the terminal alkyne with lithium bis(trimethylsilyl)amide (LHMDS) followed by treatment with trimethylborate led to the formation of an alkynylborate intermediate. Addition of *meta*-chloroperbenzoic acid (*m*CPBA) to the reaction mixture likely formed an intermediate ketene and/or mixed anhydride that was captured by the adjacent alcohol. To the best of our knowledge, this procedure for alkyne oxidation has not been reported. Hydrogenolysis of the benzyl esters followed by *in situ* acidic hydrolysis caused skeletal rearrangement to (–)-**5** in excellent yield.

Introduction of the final, deep C10 oxygen proved challenging. The steric hindrance and 'bowl' shape of **5**, in addition to its base-lability, derailed many potential solutions. **5** contains three acidic sites—the hydroxyl, the inner-lactone and the outer-lactone—but addition of 3 equivalents of strong base, followed by acidic quench at −78 °C caused significant decomposition and poor mass recovery. We found that treatment with one equivalent of potassium bis(trimethylsilyl)amide (KHMDS) followed by addition of aqueous 1M HCl caused full mass recovery, but cleanly delivered the *iso*-bilobalide scaffold (e.g. **16a**, Figure 3), a result of intramolecular translactonization[29]. Similarly, we found translactonization to occur at room temperature with 1,8-diazabicyclo[5.4.0]undec-7-ene (DBU) (bilobalide to *iso*-bilobalide, see SI section 3). This facile rearrangement is probably driven both by the proximity of the C8 hydroxyl to C4 at the Bürgi-Dunitz angle, as well as delocalization of the lactone π-system into the adjacent C-O σ* orbital. Molecular models revealed that the *iso*-bilobalide rearrangement partially folds the skeletal cavity 'inside-out' (see Figure 3) to render the inner lactone protons more accessible to reagents. However, neither the alkoxide of **1** nor its *tert*-butyldimethylsilyl (TBS) ether (**16b**) provided substantial bilobalide upon treatment with oxidant (Davis' oxaziridine, (±)-**17**). Despite the unfolding of the bilobalide cavity and C10-proton exposure (highlighted in green), base still favored deprotonation of the outer lactone and therefore oxidation provided the isomeric *neo*-bilobalide **15**. We wondered if inner lactone deprotonation required both increased exposure (rearrangement) and increased acidification. Induction through sigma bonds or delocalization of the lactone π-system into an adjacent, withdrawn C-O σ* orbital might acidify the α-protons, i.e. stabilize the corresponding enolate[30]. Conversion of **5** to the isomeric benzoate followed by deprotonation and oxidation at low temperature yielded (–)-**1** with only a trace of **15**. Combination of benzoylation and oxidation into one step proved successful, scalable and selective; *neo*-bilobalide (**11**) could not be detected.

The sequence in Figure 2 has been completed in seven days by one person to produce 0.35 g of (–)-**5**. The same overall strategy disclosed here may be applicable to *G. biloba* congeners

including the ginkgolides, some of which are glycine receptor (GlyR)-selective antagonists[31]. These studies have laid a foundation for new, enabling chemistry and a platform for functional modification of bilobalide.

Supplementary Material

Refer to Web version on PubMed Central for supplementary material.

Acknowledgments:

We thank Professors Phil Baran and Keary Engle for helpful conversations, and the Engle lab for generous donations of chiral phosphoric acids, including (–)-**B**. Professor Arnold Rheingold, Dr. Curtis Moore, and Dr. Milan Gembicky are gratefully acknowledged for X-ray crystallographic analysis. We thank Dr. Jason Chen and Brittany Sanchez in the Scripps Research Automated Synthesis Facility for purification assistance and for analysis of chiral non-racemic compounds. Generous support was provided by the National Institutes of Health (R35 GM122606) and the Uehara Memorial Foundation. Additional support was provided by Eli Lilly, Novartis, Bristol-Myers Squibb, Amgen, Boehringer-Ingelheim, the Sloan Foundation, and the Baxter Foundation.

References and Notes:

1. Dekosky ST et al. Ginkgo biloba for Prevention of Dementia: A Randomized Controlled Trial, JAMA, 300, 2253–2262 (2008). [PubMed: 19017911]
2. Wada K et al. Studies on the constitution of edible medicinal plants. Isolation and identification of 4-O-methyl-pyridoxine toxic principle from the seed of *Ginkgo biloba*, Chem. Pharm. Bull 36, 1779–1782 (1998).
3. Clarke TC, Black LI, Stussman BJ, Barnes PM, Nahin RL Trends in the use of complementary health approaches among adults: United States, 2002–2012 National health statistics reports; no 79. Hyattsville, MD: National Center for Health Statistics (2015).
4. Kiewert C et al. Role of GABAergic antagonism in the neuroprotective effects of bilobalide, Brain Res. 1128, 70–78 (2007). [PubMed: 17134681]
5. Fernandez F et al. Pharmacotherapy for cognitive impairment in a mouse model of Down syndrome, Nature Neurosci. 10, 411–413 (2007). [PubMed: 17322876]
6. Van Beek TA, Taylor LT Sample preparation of standardized extracts of *Ginkgo biloba* by supercritical fluid extraction, Phytochem. Anal 7, 185–191 (1996).
7. Lynch JW, Chen X Subunit-specific potentiation of recombinant glycine receptors by NV-31, a bilobalide-derived compound, Neurosci. Lett 435, 147–151 (2008). [PubMed: 18329806]
8. Ivic L, Sands TTJ, Fishkin N, Nakanishi K, Kriegstein AR, Strømgaard K Terpene Trilactones from *Ginkgo biloba* Are Antagonists of Cortical Glycine and $GABA_A$ Receptors, J. Biol. Chem 278, 49279–49285 (2003). [PubMed: 14504293]
9. Huang SH et al. Bilobalide, a sesquiterpene trilactone from *Ginkgo biloba*, is an antagonist at recombinant $\alpha_1\beta_2\gamma_{2L}$, Eur. J. Pharm 464, 1–8 (2003).
10. Thompson AJ, McGonigle I, Duke R, Johnston GAR, Lummis SCR A single amino acid determines the toxicity of *Ginkgo biloba* extracts, FASEB J. 26, 1884–1891 (2012). [PubMed: 22253475]
11. Nakanishi K et al. Structure of bilobalide, a rare tert-butyl containing sesquiterpenoid related to the C20-ginkgolides, J. Am. Chem. Soc 93, 3544–3546 (1971).
12. Strømgaard K, Nakanishi K Chemistry and Biology of Terpene Trilactones from *Ginkgo Biloba*, Angew. Chem. Int. Ed 43, 1640–1658 (2004).
13. Vale S Subarachnoid haemorrhage associated with *Ginkgo biloba*, Lancet 352, 36 (1998).
14. Ng CC, Duke RK, Hinton T, Johnston GAR Effects of bilobalide, ginkgolide B and picrotoxinin on $GABA_A$ receptor modulation by structurally diverse positive modulators, Eur. J. Pharm 806, 83–90 (2017).

15. Weinges K, Hepp M, Huber-Patz U, Rodewald H, Irngartinger H Chemistry of ginkgolides. 1. 10-acetyl-1-methoxycarbonyl-2,3,14,15,16-pentanorginkgolide-A, an intermediate for the synthesis of bilobalide, Liebigs Ann. Chem 1057–1066 (1986).
16. Harrison T, Myers PL, Pattenden G Radical cyclisations onto 2(5H)-furanone and maleate electrophore. An approach to the spiro- and linear-fused γ-lactone ring systems found in the ginkgolides, Tetrahedron 45, 5247–5262 (1989).
17. Emsermann J, Opatz T Photochemical approaches to the bilobalide core, Eur. J. Org. Chem 3362–3372 (2017).
18. Corey EJ, Su WG Total synthesis of a C15 ginkgolide, (±)-bilobalide, J. Am. Chem. Soc 109, 7534–7536 (1987).
19. Corey EJ, Su WG Enantioselective Total Synthesis of Bilobalide, A C15 Ginkgolide, Tetrahedron Lett. 29, 3423–3426 (1988).
20. Crimmins MT, Jung DK, Gray JL Synthetic studies on the ginkgolides: total synthesis of (±)-bilobalide, J. Am. Chem. Soc 115, 3146–3155 (1993).
21. Fernàndez-Ibáñez MÁ, Maciá B, Alonso DA, Pastor IM Recent Advances in the Catalytic Enantioselective Reformatsky Reaction, Eur. J. Org. Chem 7028–7034 (2013).
22. Wolf C, Moskowitz M Bisoxazolidine-Catalyzed Enantioselective Reformatsky Reaction, J. Org. Chem 76, 6372–6376 (2011). [PubMed: 21623640]
23. Crossley SWM, Obradors C, Martinez R Shenvi RA. Mn-. Fe-, and Co-Catalyzed Radical Hydrofunctionalizations of Olefins
24. Obradors C, Martinez RM, Shenvi RA Ph(i-PrO)SiH_2: A Remarkable Reductant for Metal-Catalyzed Hydrogen Atom Transfers, J. Am. Chem. Soc 138, 4962–4971 (2016). [PubMed: 26984323]
25. Maier G, Pfriem S, Schäfer U, Matusch R Tetra-tert-butyltetrahedrane, Angew. Chem. Int. Ed 17, 520–521 (1978).
26. González DF, Brand JP, Waser J Ethynyl-1,2-benziodoxol-3(1*H*)-one (EBX): An Exceptional Reagent for the Ethynylation of Keto, Cyano, and Nitro Esters, Chem. Eur. J 16, 9457–9461 (2010) [PubMed: 20645361]
27. Keck GE, Wagner CA The First Directed Reduction of β-Alkoxy Ktones to *anti*-1,3-Diol Monoethers: Identification of Spectator and Director Alkoxy Group, Org. Lett 2, 2307–2309 (2000). [PubMed: 10930270]
28. Julia M, Saint-Jalmes VP, Verpeaux JN Oxidation of Carbanions with Lithium *tert*-Butyl Peroxide, Synlett 3, 233–234 (1993).
29. Weinges K, Hepp M, Huber-Patz U, Irngartinger H Chemistry of ginkgolides. III. Bilobalide/isobilobalide. Structure determination by x-ray analysis, Liebigs Ann. Chem 1079–1085 (1986).
30. Byun K, Mo Y, Gao J New Insight on the Origin of the Unusual Acidity of Meldrum's Acid from ab Initio and Combined QM/MM Simulation Study, J. Am. Chem. Soc 123, 3974–3979 (2001). [PubMed: 11457147]
31. Ivic L, Sands TTJ, Fishkin N, Nakanishi K, Kriegstein AR, Strømgaard K Terpene Trilactones from *Ginkgo biloba* Are Antagonists of Cortical Glycine and $GABA_A$ Receptors, J. Biol. Chem 278, 49279–49285 (2003). [PubMed: 14504293]

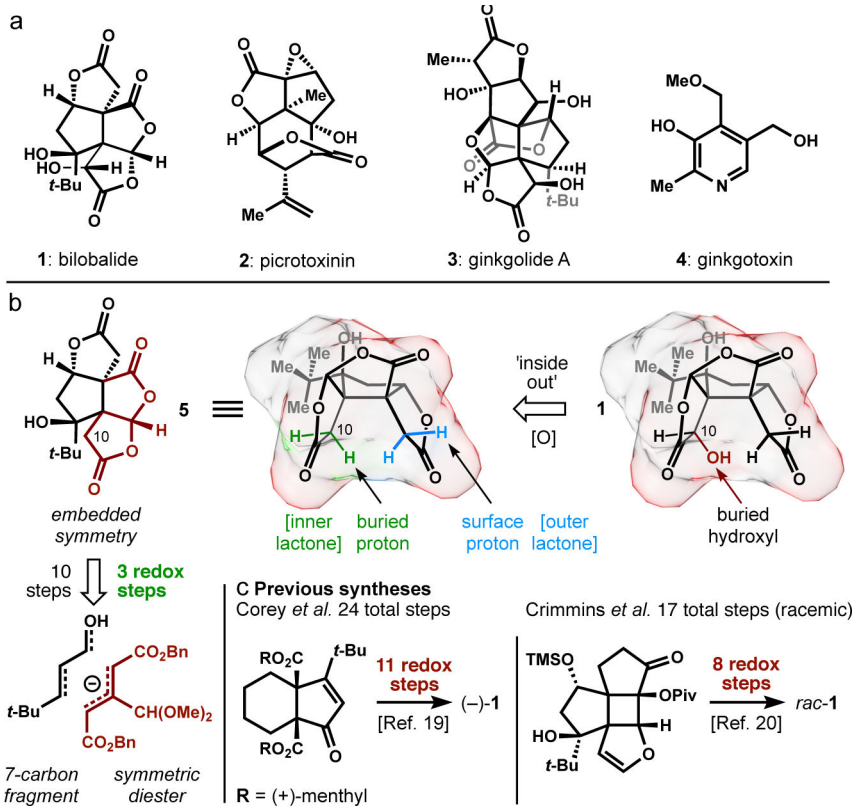

Figure 1. Congeners and design considerations.

a. Plant metabolites active in the human nervous system; **b.** late-stage excision of a buried C-H bond in bilobalide (bilobalide) allows oxygens to be placed in a symmetric starting material; **c.** prior work iteratively changed oxidation states.

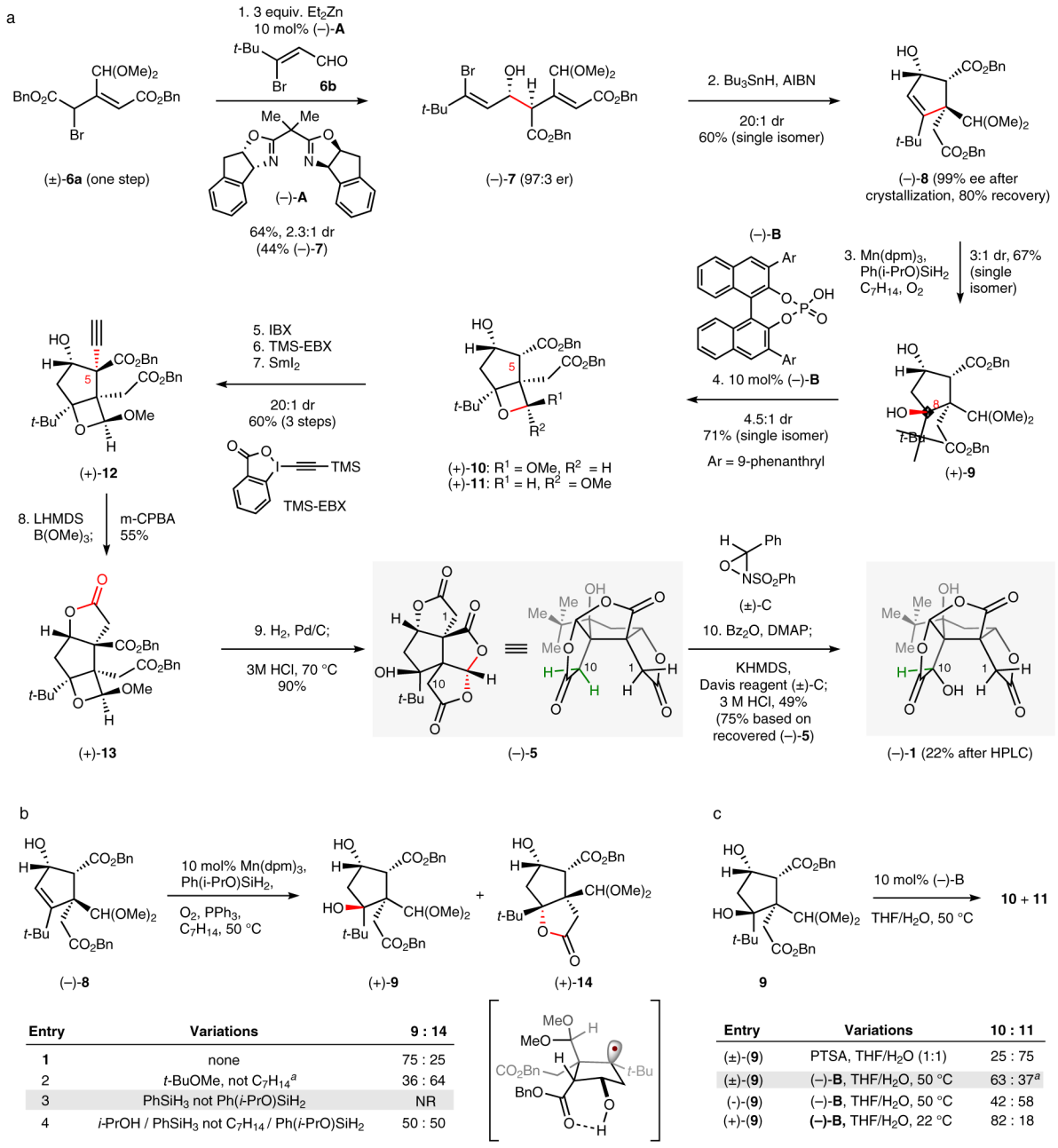

Entry	Variations	9 : 14
1	none	75 : 25
2	*t*-BuOMe, not C_7H_{14}[a]	36 : 64
3	$PhSiH_3$ not Ph(*i*-PrO)SiH_2	NR
4	*i*-PrOH / $PhSiH_3$ not C_7H_{14} / Ph(*i*-PrO)SiH_2	50 : 50

Entry	Variations	10 : 11
(±)-(**9**)	PTSA, THF/H_2O (1:1)	25 : 75
(±)-(**9**)	(–)-**B**, THF/H_2O, 50 °C	63 : 37[a]
(-)-(**9**)	(–)-**B**, THF/H_2O, 50 °C	42 : 58
(+)-(**9**)	**(–)-B,** THF/H_2O, 22 °C	82 : 18

Figure 2. Synthesis of (–)-bilobalide.

a. Reagents and conditions: (1) **6a**, **6b** (1.2 equiv.), **A** (10 mol%), Et_2Zn (3.0 equiv.), THF, −78 °C; (2) Bu_3nH (1.5 equiv.), AIBN (0.1 equiv.), PhMe, 85 °C (3) $Mn(dpm)_3$ (10 mol%), Ph(*i*-PrO)SiH_2 (3.0 equiv.), PPh_3 (1.5 equiv.), methylcyclohexane, O_2 (1 atm), 50 °C; (4) (–)-**B4** (10 mol%), THF/H_2O (2:1), 23 °C; (5) IBX (3.0 equiv.), DMSO, 23 °C; (6) TMS-EBX (3.0 equiv.), TBAF (3.0 equiv.), THF, −78 °C to −20 °C; (7) SmI_2 (8.4 equiv.), THF/H_2O (5:1), 0 °C; (8) LiHMDS (3.0 equiv.), THF, −78 °C; $B(OMe)_3$ (5.0 equiv.), 23 °C; *m*CPBA (5.0 equiv.), 0 °C; (9) H_2, Pd/C (10 wt%), MeOH, 23 °C; 3M HCl (aq.), 80 °C; (10) Bz_2O (1.5 equiv.), DMAP (1.5 equiv.), THF, 23 °C; KHMDS (3.0 equiv.), −78 °C, (±)-**C** (3 equiv.), −78 °C; 3M HCl (aq.), 80 °C; **b**. Solvent screen (enabled by Ph(^{i}PrOSiH_2); [a]C7H14

= methylcyclohexane; **c**. Acid-catalyzed oxetane acetal formation; [a]**10**: 39:61 er, **11**: 69:31 er.

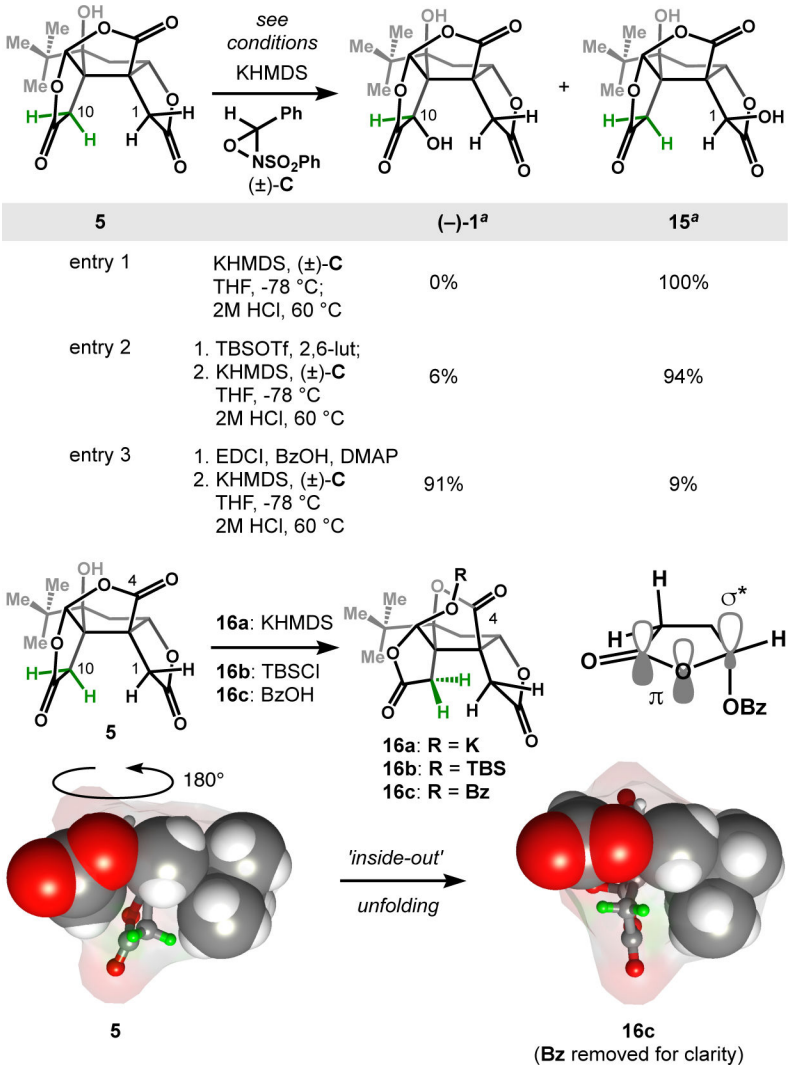

Figure 3. Late-stage, regio and stereo-selective oxidation of C10 over C1.

Reagents and conditions for entry 3: 1. EDCI (3 equiv.), BzOH (3 equiv.), DMAP (0.1 equiv.), THF; 2. KHMDS (1.5 equiv), (±)-**C** (1.5 equiv); 2M HCl, 60 °C [a] Based on conversion.